A simple fully conformal solution of Einstein's gravitational equations and the comparison of its implications with astrophysical data

Richard Dvorsky richard.dvorsky@vsb.cz

Faculty of Materials Science and Technology, Centre for Advanced Innovation Technologies
VSB – Technical University of Ostrava, 17. listopadu 15/2172, Ostrava, 708 00, Czech Republic

key words: cosmology, cosmologhical redshift, gamma-ray burst, quasars, spatial flatness, Olbers' paradox

ABSTRACT

According to general relativity, the cosmological redshift can be caused also by another mechanism, similar to the gravitational redshift of massive stars - in principle due to differences in the global metric field between a source in the past and an observer in the present. In this paper, we analyse spacetime using a fully conformal metric, where the character of natural physical time is preserved and the scaling factor acts identically on all four spacetime coordinates. Unlike the Robertson-Walker metric, the fully conformal metric preserves the time independence of the speed of light and energy-momentum tensor.

The motivation was to test the possibility of the above cosmological redshift mechanism in confrontation with astrophysical data. Probably the most important consequence is the generalized formulation and interpretation of the Hubble-Lemaître law $z(r) = (e^{Hr/c} - 1)$, which shows good agreement with astrophysical data even for farthest supernovae. Confronting the model of conformal metric with some astrophysical data shows an interesting agreement with the observed spatial distribution of astrophysical sources such as γ-ray bursts and quasars. On a cosmological scale, the fully conformal metric mentioned above naturally determines global energy density, spatial flatness, and solves the horizon problem and Olbers' paradox in infinite spacetime.

1. INTRODUCTION

According to the Standard Model, the currently accepted explanation for the cosmological redshift is a spatial expansion of the universe with an origin in the Big Bang. However, could the cosmological redshift also be interpreted as the result of a difference between the global metric field around a radiating astrophysical source in the past and the global metric field around an observer in the present?

Astrophysical data for the cosmological redshift are in most cases already published in the form of a dependence of the source receding rate on the distance from the observer. This transformation of real experimental data into terms of the preferred standard cosmological model may be misleading for the further development of the field and the above question about an alternative interpretation of the cosmological redshift was raised in the past by Fritz Zwicky [1]. However, his concept of "tired light" corresponded to a gravitational redshift based on local curvatures of spacetime by the masses of galaxies, and the redshift effect depended on local spatial distances from galactic centres. This created a problem with observational data showing a global dependence of redshift on distance from any observer.

In this paper we attempt to interpret the cosmological redshift based on the aforementioned differences in the global metric field between the two levels of spacetime. This interpretation should correspond to a global solution of Einstein's gravitational equations whose metric field varies with time $g_{\mu\nu} = g_{\mu\nu}(t)$, while at the same time ensuring full covariance of the laws of nature at every time of the space-time continuum. One of the simplest solutions that satisfies the above requirements is a flat, fully conformal Minkowski metric with time scaling $g_{\mu\nu}(t) = \psi(t) \cdot \eta_{\mu\nu}$, $g_{\mu\nu}(0) = \eta_{\mu\nu}$, where the time distance of the source t is measured into the past from the zero point $r = 0$ of the origin of the observer's coordinates. When the source radiation is observed at a distance $r = ct$ from the observer, we obtain redshift generally defined as $z = \sqrt{g_{44}(r)/g_{44}(0)} - 1 = \sqrt{g_{44}(t)/g_{44}(0)} - 1$. In this paper, the above metric is primarily derived based only on the a priori requirement of full conformality of all space-time coordinates due to the adoption of the "perfect cosmological principle" [2], [3]. Its physical meaning is then analysed in confrontation not only with cosmological redshift data, but also with some other astrophysical data.

In the field of conformal solutions of Einstein's gravitational equations, a number of mostly theoretical papers have been published [4], [5], [6], [7], [8], [9], [10], including conformal forms of the well-known Lamaitre-Friedman-Robertson-Walker (LFRW) metric [11], [12], [13], [14]. In these LFRW metrics, the Weyl conformal tensor disappears [15], which in most of these works allowed to achieve full space-time conformality by a suitable transformation of the space-time coordinates.. A comprehensive survey of these secondary conformal forms of the primary LFRW metric has been summarised by Ibison [16]. However, the primary aim of this paper is not to

derive a specific form of the fully conformal Minkowski metric per se, but to analyse its potential in describing astrophysical experimental data.

For the various variants of energy-momentum tensors in current cosmological models, most solutions of Einstein's gravitational equations are found in the assumed form of the Robertson-Walker metric with a scaling factor $a(t)$ acting only on space coordinates. By formally introducing a conformal time $d\eta = dt/a(t)$, these solutions can be transformed into the mathematical form of a fully conformal metric. Another approach, used in this paper, is to search for solutions of Einstein's gravitational equations in the form of a fully conformal metric, where the natural physical time t is preserved and the scaling factor acts equivalently on all space-time coordinates. In the case of such solutions, the covariant form of Maxwell's equations is preserved and the speed of light does not change over time (c = const.), which can be considered a positive property and a simplification within the respective models.

The fully conformal global metric with a time scaling is derived based on three premises:

PREMISE 1: Extrapolation of Einstein's gravitational equations [17] to a global cosmological scale is the correct description of the geometry of the physical universe.
PREMISE 2: The space-time structure of the universe is homogeneous and its spatial part is isotropic ("perfect cosmological principle" applies [2], [3]), and the average spatial distribution of astrophysical objects does not vary on global cosmological scales.
PREMISE 3: The local reference observer system has a Minkowski metric: $g_{\mu\nu} \rightarrow \eta_{\mu\nu}$.

Although references [2], [3] refer to the steady-state theory of the expanding universe, this paper differs significantly from that concept. Unlike these papers, the solution of Einstein's gravitational equations is sought here in the form of a fully conformal metric and not the Robertson-Walker metric. In contrast to the theoretical nature of the above papers, the fully conformal metric is confronted with astrophysical data such as the cosmological redshift and the observable spatial distribution of quasars and γ-ray bursts. On a cosmological scale, the fully conformal metric naturally determines energy density and spatial flatness, and solves the horizon problem and Olbers' paradox in infinite spacetime.

2. FULLY CONFORMAL SPACETIME WITH TIME SCALING

Let the coordinates' origin of the local inertial system (observer location), in which the microwave background of the universe is isotropic, be our "central observer point" (in next text COP). It can be located at any place and time (for simplicity let us accept the condition of local absence of gravitational bodies). Taking into account the experimentally confirmed spatial flatness in the vicinity of the COP, we establish Minkowski coordinates $\boldsymbol{x_o} = (x_{o1}, x_{o2}, x_{o3}, x_{o4} = ct_o)$ with own time t_o for this local inertial system with the origin just at the COP. Since the real universe allows for an infinite number of alternative COPs, for the following analysis we restrict ourselves to a single COP at the origin of the above local Minkowski coordinate system $\boldsymbol{x_o} = (x_{o1}, x_{o2}, x_{o3}, x_{o4} = ct_o)$. This local Minkowski coordinate system near the origin merges with the general curvilinear global coordinate systém $\boldsymbol{x} = (x_1, x_2, x_3, x_4 = ct)$, which is used to locate points on a whole variety of the corresponding spacetime, and which parametrizes its global metric field $g_{\mu\nu}(\boldsymbol{x})$. All further considerations are based on PREMISE 1, PREMISE 2 and PREMISE 3 above.

Let us find solutions of Einstein's gravitational equations without a cosmological constant in the form of a fully conformal Minkowski metric $\eta_{\mu\nu}$ with purely temporal global scaling $\psi(x_4)$

$$R_{\mu\nu} - \frac{1}{2} R g_{\mu\nu} = \kappa T_{\mu\nu} \quad \cdots \quad \begin{cases} g_{\mu\nu}(x_4) \overset{\text{def}}{=} \psi(x_4)\eta_{\mu\nu} = \psi(x_4) \begin{pmatrix} 1 & 0 & 0 & 0 \\ 0 & 1 & 0 & 0 \\ 0 & 0 & 1 & 0 \\ 0 & 0 & 0 & -1 \end{pmatrix} \\ ds^2 = g_{\mu\nu}(x_4) dx_\mu dx_\nu = \psi(x_4)\left(dx_1^{\,2} + dx_2^{\,2} + dx_3^{\,2} - dx_4^{\,2} \right) \end{cases} \tag{1}$$

From the corresponding Christoffel symbols $\Gamma^{\mu}{}_{\nu\lambda}$ as functions of single time variable x_4, only the following functions are nonzero for the conformal metric tensor (1) APPENDIX 1.:

$$\Gamma^{\mu}{}_{\nu\lambda}(x_4)=\frac{1}{2}g^{\mu\alpha}(x_4)\left(\partial_\nu g_{\alpha\lambda}(x_4)+\partial_\lambda g_{\alpha\nu}(x_4)-\partial_\alpha g_{\nu\lambda}(x_4)\right) \quad . \tag{2}$$

$$\left.\begin{aligned}\Gamma^{1}{}_{14}(x_4)&=\Gamma^{1}{}_{41}(x_4)\\ \Gamma^{2}{}_{24}(x_4)&=\Gamma^{2}{}_{42}(x_4)\\ \Gamma^{3}{}_{34}(x_4)&=\Gamma^{3}{}_{43}(x_4)\\ \Gamma^{4}{}_{11}(x_4)=\Gamma^{4}{}_{22}(x_4)&=\Gamma^{4}{}_{33}(x_4)=\Gamma^{4}{}_{44}(x_4)\end{aligned}\right\}=\frac{1}{2}\partial_4\ln\psi(x_4)$$

The following Ricci tensor is non-zero only in the diagonal components, and the scalar curvature R is also a non-zero function of single time variable x_4 APPENDIX 3.

$$\begin{aligned}R_{11}&=R_{22}=R_{33}=\frac{1}{2}\partial_4{}^2\ln\psi(x_4)+\frac{1}{2}\left(\partial_4\ln\psi(x_4)\right)^2\\ R_{44}&=-\frac{3}{2}\partial_4{}^2\ln\psi(x_4)\\ R&=\left(-3\partial_4{}^2\ln\psi(x_4)-\frac{3}{2}\left(\partial_4\ln\psi(x_4)\right)^2\right)\psi^{-1}(x_4)\end{aligned} \quad . \tag{3}$$

While the purely spatial part of the 3D has the character of a flat space E3 [18], the total global curvature R of the spacetime according to (1) is generally non-zero.

In a uniform (homogeneous and spacial isotropic) universe, the energy-momentum tensor $T_{\mu\nu}$ on a global cosmological scale can be approximated by a model of inert incoherent dust (particulate matter) with energy density ε_p uniformly dispersed in an ideal static space-time fluid with energy density ε_s and global pressure p. With respect to PREMISE 2, all the parameters mentioned are independent of time.

$$T_{\mu\nu}=\underbrace{\begin{pmatrix}0&0&0&0\\0&0&0&0\\0&0&0&0\\0&0&0&\varepsilon_p\end{pmatrix}}_{T^{par}{}_{\mu\nu}}+\underbrace{\begin{pmatrix}p&0&0&0\\0&p&0&0\\0&0&p&0\\0&0&0&\varepsilon_s\end{pmatrix}}_{T^{spa}{}_{\mu\nu}}\rightarrow T_{\mu\nu}=\begin{pmatrix}p&0&0&0\\0&p&0&0\\0&0&p&0\\0&0&0&\left(\varepsilon_p+\varepsilon_s\right)\end{pmatrix}. \tag{4}$$

While the $T^{par}{}_{\mu\nu}$ tensor corresponds to localised particulate forms of energy, such as gases, dust and stars, the $T^{spa}{}_{\mu\nu}$ tensor corresponds to the global energy structure of a continuous metric space-time field. After substituting the energy-momentum tensor (4) into (1), we obtain conditions for a currently unknown scaling function $\psi(x_4)$ APPENDIX 4.

$$R_{\mu\nu}-\frac{1}{2}Rg_{\mu\nu}=\kappa T_{\mu\nu}\rightarrow\left\{\begin{aligned}R_{11}-\frac{1}{2}R\psi(x_4)\eta_{11}&=\kappa p\\ R_{22}-\frac{1}{2}R\psi(x_4)\eta_{22}&=\kappa p\\ R_{33}-\frac{1}{2}R\psi(x_4)\eta_{33}&=\kappa p\end{aligned}\right\}\rightarrow\boxed{-\partial_4{}^2\left[\ln\psi(x_4)\right]-\frac{1}{4}\left(\partial_4\left[\ln\psi(x_4)\right]\right)^2=\kappa p}\ \text{(a)}$$

$$R_{44}-\frac{1}{2}R\psi(x_4)\eta_{44}=\kappa\varepsilon\rightarrow\boxed{\frac{3}{4}\left(\partial_4\left[\ln\psi(x_4)\right]\right)^2=\kappa\left(\varepsilon_p+\varepsilon_s\right)}\quad\text{(b)} \tag{5}$$

The solution of equation (5)-(b) gives a general form of the scaling function $\psi(x_4)$

$$\psi_{\pm}(x_4)=\psi(0)e^{\pm x_4\sqrt{\frac{4}{3}\kappa\left(\varepsilon_p+\varepsilon_s\right)}}. \tag{6}$$

The problem of alternatives $\psi_{-}(x_4)$ and $\psi_{+}(x_4)$ of the scaling function (6) will be discussed below. With respect to PREMISE 3, the scaling function (6) becomes:

$$\psi(0)=1\ \rightarrow\ \psi_{\pm}(x_4)=e^{\pm x_4\sqrt{\frac{4}{3}\kappa\left(\varepsilon_p+\varepsilon_s\right)}}. \tag{7}$$

At this stage, the exponent contains an as yet unspecified total density of homogeneously distributed energy $(\varepsilon_p+\varepsilon_s)$. The formulation of the scaling function (7) will be confronted with the present cosmological redshift data in the next section to provide a concrete form of the conformal metric tensor (1).

3. COSMOLOGICAL REDSHIFT

Let us analyse the relative time flow at different radial distances from the COP. The spacetime interval $ds(\boldsymbol{x})$ is a function of the four-vector $\boldsymbol{x}(x_1, x_2, x_3, x_4)$ due to the generally varying metric tensor $g_{\mu\nu}(\boldsymbol{x})$. Similarly, the differentials of the proper Minkowski coordinates $(x_{o1}(\boldsymbol{x}), x_{o2}(\boldsymbol{x}), x_{o3}(\boldsymbol{x}), x_{o4}(\boldsymbol{x}))$ of the local inertial systems around any point $\boldsymbol{x}$ of spacetime, are a function of the four-vector $\boldsymbol{x}$

$$g_{\mu\nu}(\boldsymbol{x})dx_\mu dx_\nu = ds(\boldsymbol{x})^2 = \eta_{\mu\nu}dx_{o\mu}(\boldsymbol{x})dx_{o\nu}(\boldsymbol{x})$$

$$ds(\boldsymbol{x})^2 = \underbrace{g_{11}(\boldsymbol{x})dx_1^2}_{\eta_{11}dx_{o1}(\boldsymbol{x})^2} + \underbrace{g_{22}(\boldsymbol{x})dx_2^2}_{\eta_{22}dx_{o2}(\boldsymbol{x})^2} + \underbrace{g_{33}(\boldsymbol{x})dx_3^2}_{\eta_{33}dx_{o3}(\boldsymbol{x})^2} + \underbrace{g_{44}(\boldsymbol{x})dx_4^2}_{\eta_{44}dx_{o4}(\boldsymbol{x})^2} \quad . \tag{8}$$

If the chosen position of the COP in spacetime is denoted by $\boldsymbol{x}(0, 0, 0, 0) \equiv \boldsymbol{0}$, then the Minkowski coordinates $(x_{o1}(\boldsymbol{0}), x_{o2}(\boldsymbol{0}), x_{o3}(\boldsymbol{0}), x_{o4}(\boldsymbol{0}))$ of the corresponding local inertial system in the conformal metric (1) according to (7), coincide with the geodetic coordinates (x_1, x_2, x_3, x_4) in the vicinity of $\boldsymbol{0}$ (which is consistent with the Minkowski metric of the surrounding spacetime, confirmed by experimental experience - 3D-spatial flatness and a large region with negligible cosmological redshift)

$$ds(\boldsymbol{0})^2 = \underbrace{g_{11}(\boldsymbol{0})}_{\eta_{11}}\underbrace{dx_1^2}_{dx_{o1}(\boldsymbol{0})^2} + \underbrace{g_{22}(\boldsymbol{0})}_{\eta_{22}}\underbrace{dx_2^2}_{dx_{o2}(\boldsymbol{0})^2} + \underbrace{g_{33}(\boldsymbol{0})}_{\eta_{33}}\underbrace{dx_3^2}_{dx_{o3}(\boldsymbol{0})^2} + \underbrace{g_{44}(\boldsymbol{0})}_{\eta_{44}}\underbrace{dx_4^2}_{dx_{o4}(\boldsymbol{0})^2} \quad . \tag{9}$$

There is a well-known formula for the own time flow τ in a point event ($dx_i = 0$, i = 1,2,3) at the COP $\boldsymbol{0}$ at any point $\boldsymbol{x}$ in spacetime [19], [15]

$$\left.\begin{aligned}\eta_{44}dx_{o4}(\boldsymbol{x})^2 &= g_{44}(\boldsymbol{x})dx_4^2\\ \eta_{44}dx_{o4}(\boldsymbol{0})^2 &= g_{44}(\boldsymbol{0})dx_4^2\end{aligned}\right\} \rightarrow dx_{o4}(\boldsymbol{x}) = dx_{o4}(\boldsymbol{0})\sqrt{\frac{g_{44}(\boldsymbol{x})}{g_{44}(\boldsymbol{0})}} \rightarrow dt_o(\boldsymbol{x}) = dt_o(\boldsymbol{0})\sqrt{\frac{g_{44}(\boldsymbol{x})}{g_{44}(\boldsymbol{0})}}. \tag{10}$$

Within the conformal metric (1), the (10) takes the form of

$$dt_o(\boldsymbol{x}) = dt_o(\boldsymbol{0})\sqrt{\frac{\eta_{44}\psi(x_4)}{\eta_{44}}} \quad \rightarrow \quad dt_o(x_4) = dt_o(0)\sqrt{\psi(x_4)}. \tag{11}$$

As a result of the assumption of the conformal metric (1) and relation (7), the equation (11) takes the form

$$dt_o(x_4) = dt_o(0)\sqrt{\psi_\pm(x_4)} = dt_o(0)e^{\pm x_4\sqrt{\frac{\kappa}{3}(\varepsilon_p+\varepsilon_s)}}. \tag{12}$$

The negative time coordinate $x_4 \le 0$ of the past defines a radial "observation sphere with positive radius" r (13) with respect to the COP

$$\left.\begin{aligned}dr^2 &= dx_1^2 + dx_2^2 + dx_3^2\\ ds(x_4)^2 &= 0\end{aligned}\right\} \rightarrow \psi(x_4)dr^2 - \psi(x_4)dx_4^2 = 0 \rightarrow dr = -dx_4 \rightarrow r = -x_4. \tag{13}$$

If two different points emit light from a source with the same frequency $\nu(0)$, then we measure an identical value of $\nu(0) \sim 1/dt_o(0)$ for a source at $r = 0$ near the COP, while for a source at a large distance r the measured frequency $\nu(r) \sim 1/dt_o(r)$ will theoretically be higher or lower depending on the polarity of the exponent in (12)

$$\nu(r) = \nu(0)e^{\mp r\sqrt{\frac{\kappa}{3}(\varepsilon_p+\varepsilon_s)}}. \tag{14}$$

At this stage, the polarity of the exponent (14) can be decided based on experimental experience. Since a positive sign would represent a blue cosmological shift, it is appropriate to see it as "non-physical" for now, but this does not exclude its possible meaning in the future. On the contrary, a red cosmological shift ($\nu(r) < \nu(0)$) has been clearly confirmed experimentally, and therefore we will currently accept only the negative sign

$$\nu(r) = \nu(0)e^{-r\sqrt{\frac{\kappa}{3}(\varepsilon_p+\varepsilon_s)}} \quad . \tag{15}$$

Let's reformulate the (15) to the "redshift" equation (16)

$$z \overset{\text{def}}{=} \frac{\nu(0)-\nu(r)}{\nu(r)} \quad \rightarrow \quad z = e^{r\sqrt{\frac{\kappa}{3}(\varepsilon_p+\varepsilon_s)}} - 1, \tag{16}$$

which converges into the familiar linear form for small values of the exponent (small distances r from the COP)

$$z = \left(e^{r\sqrt{\frac{\kappa}{3}(\varepsilon_p+\varepsilon_s)}} \approx r\sqrt{\frac{\kappa}{3}(\varepsilon_p+\varepsilon_s)} + 1\right) - 1 \rightarrow z = \left[\sqrt{\frac{\kappa}{3}(\varepsilon_p+\varepsilon_s)}\right]r. \tag{17}$$

Equation (17) is formally equivalent to a linear formulation of the standard Hubble–Lemaître law for small cosmological distances

$$z = \frac{H}{c} r . \tag{18}$$

Combining (17) and (18), we get a final form that allows us to directly calculate the equivalent mass density of the universe ($\rho_p + \rho_s$). Its value corresponds to the critical density ρ_{crit} [20] for the flat space solution of the Friedmann model

$$\left.\begin{aligned} \frac{H}{c} &= \sqrt{\frac{\kappa}{3}\left(\varepsilon_p + \varepsilon_s\right)} \\ \kappa &= \frac{8\pi G}{c^4} \end{aligned}\right\} \rightarrow \rho_p + \rho_s = \frac{3H^2}{8\pi G} = \rho_{\text{crit}} = 8 \cdot 10^{-27}\ \text{kgm}^{-3} \rightarrow \boxed{\nu(r) = \nu(0) e^{-\frac{H}{c} r}} . \tag{19}$$

Based on this match (19), the equation (16) can be expressed as the final form of the generalized Hubble–Lemaître law

$$\boxed{z = e^{\frac{H}{c} r} - 1} . \tag{20}$$

Its nonlinear character is clearly visible only at large cosmological distances r (see Fig.1)

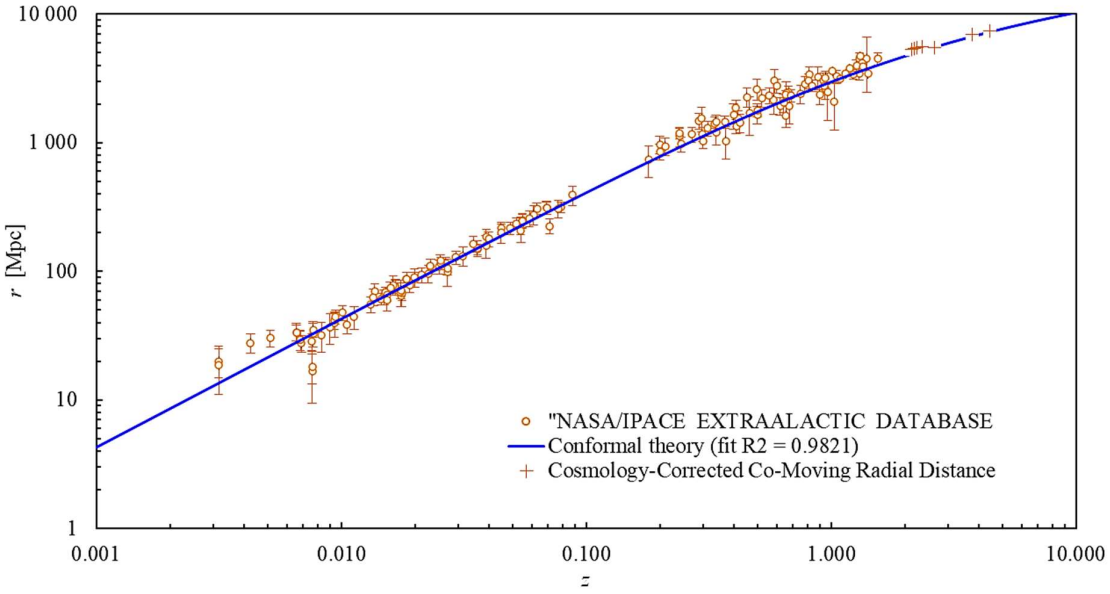

Fig.1 Hubble–Lemaître diagram - experimental points are taken from NASA/IPACE EXTRAGALACTIC DATABASE [21] and the blue curve —— represents the fit of the generalized Hubble–Lemaître law (20) for the Hubble's parameter 69.7 [kms^{-1}/Mpc] [22].

The coefficient of determination $R^2 = 0.9821$ of the fit in Fig. 1 documents a good agreement with the experimental data and confirms the realistic nature of the mathematical formula of the generalized Hubble–Lemaître law (20). In this situation, it is worth pointing out that its nonlinearity is a direct consequence of the conformal solution of Einstein's gravitational equations (1) without the cosmological term and it does not require the hypothetical concept of dark energy. Based on relations (17) and (18), the scaling function (7) and hence the metric tensor $g_{\mu\nu}$ takes a concrete form

$$\left.\begin{aligned} \psi(x_4) &= e^{x_4\sqrt{\frac{4}{3}\kappa\left(\varepsilon_p + \varepsilon_s\right)}} \\ \frac{H}{c} &= \sqrt{\frac{\kappa}{3}\left(\varepsilon_p + \varepsilon_s\right)} \end{aligned}\right\} \rightarrow \psi(x_4) = e^{2\frac{H}{c} x_4} \rightarrow \boxed{g_{\mu\nu}(x_4) = e^{2\frac{H}{c} x_4} \eta_{\mu\nu}} , \left\{\begin{aligned} &\text{past: } x_4 < 0 \\ &\text{COP: } x_4 = 0 \\ &\text{future: } x_4 > 0 \end{aligned}\right\} . \tag{21}$$

The global spacetime determined by the metric tensor (21) is the fundamental background of the geometrical universe on a cosmological scale. Due to the non-linear nature of Einstein's equations, the "composition" of local gravitational fields is not simply additive with the above cosmological background. For example, the flat Minkowski spacetime $\eta_{\mu\nu}$ can be replaced by a conformal metric (21) in the asymptotic limit of the Schwarzschild field for $r \rightarrow \infty$, but in the vicinity of a source of mass it is problematic to separate those two metric factors. This

non-trivial situation is closely related to the still debated problem of whether cosmological expansion also occurs on a local scale in gravitationally bound systems.

4. SPATIAL DISTRIBUTION OF γ-RAY BURSTS

Another cosmological test of the conformal Minkowski metric hypothesis can be an experimental verification of the natural homogeneous distribution of matter on a global cosmological scale. Such a test can be performed by observing highly specific astrophysical objects and events such as black holes, quasars, and ultimately γ-ray sources that can be understood as standards (the distribution of galaxies is inappropriate for such a test due to their highly non-standard diversity).

We will discuss the spatial distribution of γ-ray bursts in the following chapter. In [23] and [24] they published a methodology for applying the $V/V_{\max}$ test to γ-ray sources and subsequently performed a constrained analysis of the spatial distribution for 140 sources [25]. The result shows an increasing deficit in the observed number of low intensity sources. Assuming an identical nature of the sources and the standard Euclidean flat-space metric E3, these results can be interpreted as a decrease in source density towards the past within a fully conformal spacetime. Such an interpretation leads to the conclusion that the γ-ray density changes over time on a global scale.

Let us now perform a similar analysis under a hypothetical conformal metric. The time-independent nature of the energy-momentum tensor (4) requires a global density of γ-ray sources invariant over time. The number of sources N within in a sphere of radius $r_{\max}$ around the COP is given by the time-invariant global source density $n_{\gamma o}$:

$$N\left(r_{\max}\right) = n_{\gamma o}\frac{4}{3}\pi {r_{\max}}^3. \tag{22}$$

In the mentioned $V/V_{\max}$ test [23], the ratio of the intensity $C_{\max} = C(r_{\max})$ of the farthest detected source at distance $r_{\max}$ to the threshold intensity $C_{\min} = \min C$ at the detection limit is chosen as the independently variable distribution parameter. The intensity of the source $C_{\max}$ decreases not only with the inverse square of the distance $r_{\max}$ but also due to the conformal metric (21). As a result, the intensity on a model source surface of radius R decreases with distance $r_{\max}$ from the observer.

Now we analyse the measurement of the "observed intensity" C [$\mathrm{Jm^{-2}s^{-1}}$] at distant sources, taking into account the effect of the conformal metric (21). For simplicity, consider a spherical radiation source of radius R. Let us denote by $C_o(R)$ the surface intensity of the radiation in its local inertial system (x_{o1}, x_{o2}, x_{o3}, x_{o4}) (8) and then denote by $C(R)$ the same relative surface intensity of the radiation in the global system (x_1, x_2, x_3, x_4) (8) of the COP at distance r. While the intensity $C(r)$ observed in the COP decreases according to the standard $C(r) \sim 1/r^2$ dependence, the transition between the $C_o(R) \rightarrow C(R)$ intensities is due to the effect of the conformal metric (21) on the intrinsic surface intensity $C_o(R)$. With a suitable orientation of $x_1 = r$, the remaining two space coordinates x_2 and x_3 define a plane perpendicular to the line between source and the COP. The two surface differentials dS_o and dS of the source surface then lie in this plane, radiating towards the COP, and the relation $C_o(R) \rightarrow C(R)$ can be written as

$$\left.\begin{aligned} C_0\left(R\right) &\overset{\text{def}}{=} \frac{d^2E}{dS_o dt_o} \\ dS_o &= dx_{o2}dx_{o3} \\ C\left(R\right) &\overset{\text{def}}{=} \frac{d^2E}{dSdt} \\ dS &= dx_2 dx_3 \end{aligned}\right\} \rightarrow C\left(R\right) = C_0\left(R\right)\frac{dS_o dt_o}{dSdt}. \tag{23}$$

As a consequence of the (8), (13) and the conformal metric (21) we can write

$$\left.\begin{aligned} dx_{o\mu}\left(x_4\right) &= e^{\frac{H}{c}x_4}dx_\mu \\ x_4 &= -r \end{aligned}\right\} \rightarrow \left\{\begin{aligned} dx_{o4} &= e^{-\frac{H}{c}r}dx_4 \rightarrow dt_o = e^{-\frac{H}{c}r}dt \\ dS_o &= dx_{o1}dx_{o2} = e^{-2\frac{H}{c}r}dx_1 dx_2 = e^{-2\frac{H}{c}r}dS \end{aligned}\right\} \rightarrow \frac{dS_o dt_o}{dSdt} = e^{-3\frac{H}{c}r}, \tag{24}$$

and for the relative radiation intensity (23) on a model source surface of radius R it is

$$C\left(R\right) = C_o\left(R\right)e^{-3\frac{H}{c}r_{\max}}. \tag{25}$$

As a result of the simultaneous decrease in intensity with the square of the distance, equation (25) takes its final form:

$$\underbrace{C\left(r_{\max}\right)}_{C_{\max}}\cdot\left(4\pi {r_{\max}}^2\right) = C\left(R\right)\cdot\left(4\pi R^2\right) \rightarrow C_{\max} = C_o\left(R\right)\frac{R^2}{{r_{\max}}^2}e^{-3\frac{H}{c}r_{\max}}. \tag{26}$$

The NSSTC, BATSE4B astrophysical database [26] contains data as dependence of the number of sources on the ratio of the minimum intensity to the threshold intensity $N(C_{max}/C_{min})$. To test the conformal metric hypothesis (1), (21), we express equation (26) in terms of an intensity ratio

$$\frac{C_{\max}}{C_{\min}} = \left(C_o\left(R\right)\frac{R^2}{C_{\min}} \right) e^{-3\frac{H}{c}r_{\max}} \left(r_{\max}\right)^{-2}. \tag{27}$$

The mutual dependence of the two parameters then comes from the simultaneous validity of (22) and (27):

$$\left\{ \begin{array}{l} A = \left(\frac{C_o\left(R\right)}{C_{\min}} R^2 \right) \left(\frac{3}{4\pi n_{\gamma o}} \right)^{-\frac{2}{3}} \left[-\right] \\ B = 3\frac{H}{c} \left(\frac{3}{4\pi n_{\gamma o}} \right)^{\frac{1}{3}} \left[-\right] \end{array} \right\} \quad \rightarrow \quad \boxed{\frac{C_{\max}}{C_{\min}} = AN^{-\frac{2}{3}} e^{-BN^{\frac{1}{3}}}} \tag{28}$$

The fit of the theoretical dependence (28) to the mentioned experimental data of NSSTC, BATSE4B [26] is shown in Fig. 2.

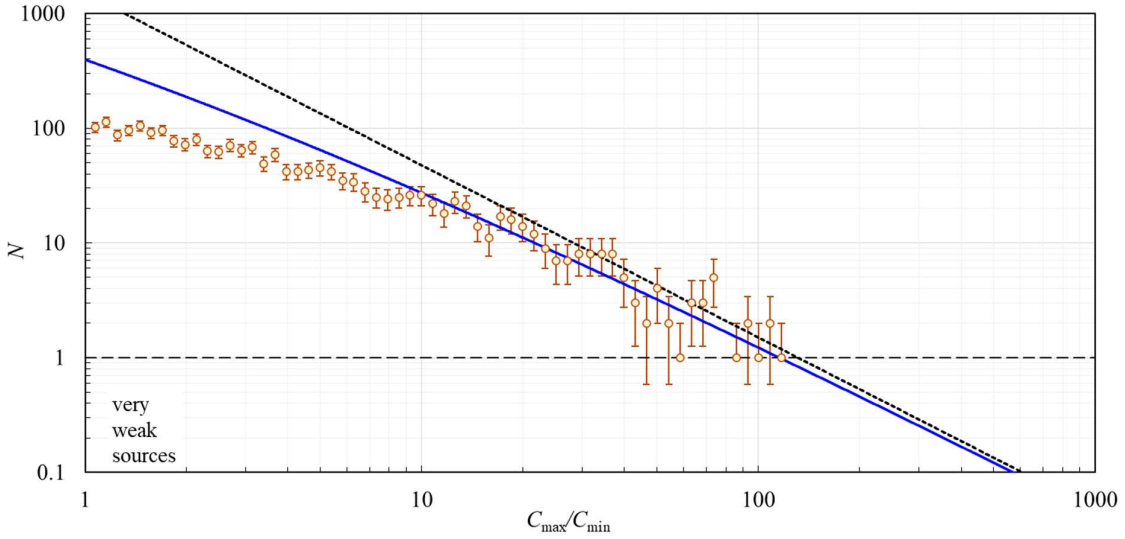

Fig. 2 Theoretical fit — distribution of the total number N of γ-ray burst sources as a function of the C_{max}/C_{min} ratio for 2372 measured sources (A = 130, B = 0.12). The black dashed line would correspond to a uniform distribution of sources in flat space with the standard Euclidean metric E3, as indicated by a formal extrapolation of the plot below the single-source detection level of N = 1.

The first requirement of the fit is the limit transition $B \rightarrow 0$ of formula (28) to the standard version of the Minkowski metric for small distances from the COP, which shows asymptotic behaviour for well-detectable sources with large C_{max} corresponding to smaller r_{max}. The fit has a coefficient of determination $R^2 \approx 0.888$ in the region $C_{max}/C_{min} \geq 10$. The above fit for $B = 0.12$ gives a time-invariant global γ-ray burst density of $n_{\gamma o} \approx 1.47 \cdot 10^{-75}$ m^{-3} $\approx$ 43 Gpc^{-3} according to (28).

The detection of the vast majority of strong sources in the nearby region is highly probable both in terms of their high intensity and their frequency of occurrence in a relatively small volume of the vicinity of the COP. However, in more distant regions, the detection probability is negatively affected both by the decreasing intensity of the sources and by their more difficult localization in an extremely increasing volume. In the Gaussian angular distribution of the intensity of narrow γ-ray bursts [27], the minimum measurable intensity C_{min} determines the edge of the Gaussian profile, so the effective solid angle detection of the γ -ray burst decreases with distance. This naturally reduces the probability of passage through the ground-based observation point and hence the frequency of detected sources. Detection of "missing" sources could therefore serve as one way to verify or falsify this hypothesis of a global conformal metric of the universe.

5. SPATIAL DISTRIBUTION OF QUASARS

D. Sciama and M. Rees published a paper in 1966 [28] with the intention of falsifying the steady state theory of the universe. The paper showed that the frequency of observed quasars depends on the magnitude of the redshift, and from this fact he deduced a time evolution of the source density that contradicts the ideas of the steady-state model of the universe. This raises the question of how to correctly interpret observations of sources with different redshift values. Although the estimated time evolution of the source density was contrary to steady-state concepts, it has not been explained in principle even within the standard ΛCMD cosmological model. It is associated with the general assumption of the genesis and evolution of astrophysical objects within any cosmological theory with a time origin. Of course, the time evolution cannot be excluded even in models without said beginning, because with limited observational experience, we may miss slow global processes. ("Too brief glimpse into the past from the beginning of summer may lead one to believe that the world was created in winter").

Thus, we examine whether the hypothesis of the conformal metric is consistent with the assumption that the distribution of quasars seems to be homogeneous in space from the COP. For a time-invariant global source density n_{qo}, the number of sources dN contained in a differential spherical shell of radius r around the COP is given by

$$dN = n_{qo} 4\pi r^2 dr \,. \tag{29}$$

Now we derive the distribution of dN/dz as a function of redshift from all observed quasars. From the generalized Hubble–Lemaître law (20), the radial parameters r and dr on the left-hand side of equation (29) can be expressed as a function of the redshift z

$$z = e^{\frac{H}{c}r} - 1 \quad \rightarrow \quad \begin{cases} r = \dfrac{c}{H}\ln\left(z+1\right) \\ \dfrac{dz}{dr} = \dfrac{H}{c}e^{\frac{H}{c}r} \rightarrow dr = \dfrac{c}{H}e^{-\frac{H}{c}r}dz \rightarrow dr = \dfrac{c}{H}\dfrac{dz}{z+1} \end{cases} . \tag{30}$$

Substitution into (29) then gives the final formula for comparison with experimental data

$$A = 4\pi n_{qo}\left(\frac{c}{H}\right)^3 \quad \rightarrow \quad \boxed{\frac{dN}{dz} = A\frac{\left(\ln\left(z+1\right)\right)^2}{z+1}} \,. \tag{31}$$

The relevant data were used from The Million Quasars (Milliquas) catalog, v7.2aa, 18 October 2021 [29], which contains experimental data obtained by observing about 977 000 sources. The fit of the theoretical dependence (31) to these experimental data is shown in Fig. 3.

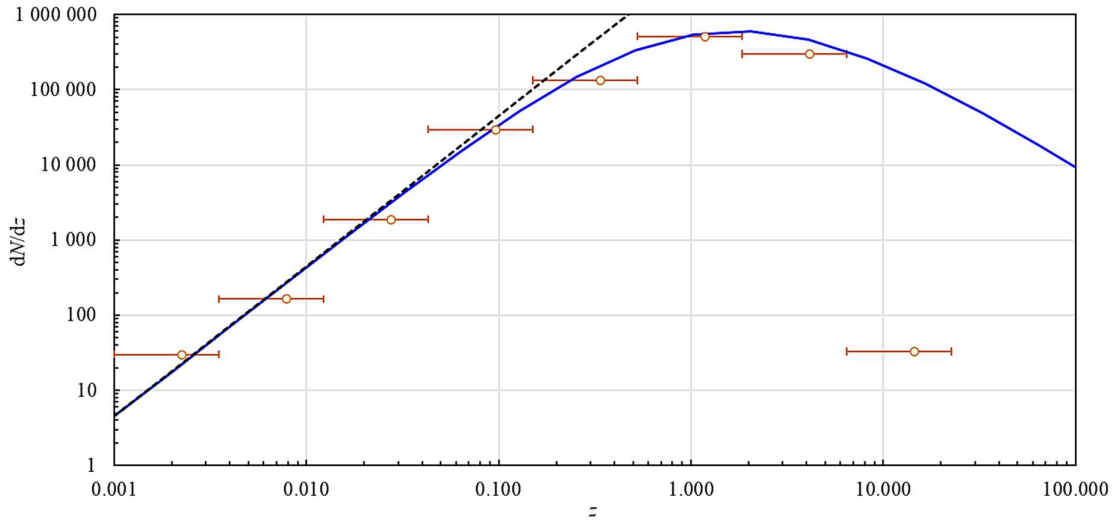

Fig.3 Theoretical fit —— of the dependence of the number of quasars with the increase in redshift dN/dz on the magnitude of their redshift z (for parameter $4.5{\cdot}10^6$) [29]. Hollow points correspond to the average of all measured z values within respective interval and horizontal line define its width. The black dashed line corresponds to a uniform distribution of sources in flat space with Euclidean metric E3 and the standard linear form of Hubble–Lemaître law for redshift.

The requirement of the fit is again the limit transition $z \rightarrow 0$ of equation (31) to the standard version of the Minkowski metric at small distances from the COP. This requirement of asymptotic behaviour is satisfied by the transition of the function (31) to the standard form z^2. The theoretical shape of the fit function is confronted in good agreement with the number of quasars in the first six statistical intervals, which are shown in Fig. 3 as

horizontal lines. The calculated coefficient of determination $R^2 \approx 0.9511$ for the first six points characterise a partial agreement between theory and experiment. Using the regression parameter $A \approx 4.5 \cdot 10^6$ in equation (31) we can estimate the quasar number density in the universe to $n_{qo} \approx 1.55 \cdot 10^{-73}$ m^{-3} $\approx$ 4559 Gpc^{-3}.

Similarly to the previous section, we can also justify the deficit in the number of sources in the last interval for high values of z. And again, additional measurements could serve to partially verify, or refute the hypothesis of a global conformal metric of the universe.

6. OLBERS' PARADOX AND THE OBSERVABLE UNIVERSE

The assumption of a luminous sky in the visible light region does not match experimental experience (Olbers' paradox), and in a universe with a fully conformal metric (1) this paradox can be explained via redshift. Assume that on sufficiently large cosmological scales the number density of model astrophysical light sources n can be approximated by a constant. We introduce the intensity contribution dI_Ω of the average model sources from the differential volume $dV = d\Omega r^2 dr$ at distance r from the COP, oriented towards the COP, which is given by the emission of radiative energy ε from the source surface to the differential solid angle $d\Omega$

$$dI_\Omega(r) = \left\{ \frac{d^2\varepsilon(r)}{dt(r)dS(r)} \right\} n d\Omega r^2 dr \,. \tag{32}$$

As a result of the metric transformation of the derivative variables (24), it decreases exponentially with distance r from the COP

$$\left\{ \frac{dt(0)dS(0)}{dt(r)dS(r)} = e^{-3\frac{H}{c}r} \right\} \rightarrow dI_\Omega(r) = \left\{ \frac{d^2\varepsilon(r)}{dt(0)dS(0)} \right\} e^{-3\frac{H}{c}r} n d\Omega r^2 dr \,. \tag{33}$$

For simplicity of the model derivation, assume purely thermal emission from an average model source with surface temperature $T(0)$. After including all the mentioned effects, the intensity contribution dI_Ω (33) takes the form

$$\left. \begin{array}{l} \text{inverse square law} \rightarrow \dfrac{d^2\varepsilon(r)}{dt(0)dS(0)} = \left(\dfrac{\sigma}{\pi} T(r)^4 \right) \dfrac{1}{r^2} \\ \text{redshift+Wien's law} \rightarrow \dfrac{T(r)}{T(0)} = \dfrac{\nu_{\max}(r)}{\nu_{\max}(0)} = e^{-\frac{H}{c}r} \end{array} \right\} \rightarrow dI_\Omega(r) = \left(\frac{\sigma}{\pi} T(0)^4 \right) e^{-7\frac{H}{c}r} n d\Omega dr \,. \tag{34}$$

The experimentally measured intensity $I_\Omega(R)$ [Wm^{-2}sr^{-1}] in the direction of the unit angle axis is the sum of all contributions from the opposite half-space 2π to the distance R of the observation horizon

$$I_\Omega(R) = \iiint\limits_{V_R^{2\pi}} dI_\Omega = \int\limits_0^{2\pi} \int\limits_0^R \left(\frac{\sigma}{\pi} T(0)^4 \right) e^{-7\frac{H}{c}r} n d\Omega dr = 2\pi \left(\frac{\sigma}{\pi} T(0)^4 \right) n \left(\int\limits_0^R e^{-7\frac{H}{c}r} dr \right). \tag{35}$$

Without knowledge of the model parameters n and $T(0)$, the dependence of the intensity $I_\Omega(R)$ on the distance R from the COP can be characterized by the function $\Phi(R)$, which is defined by the parametric integral in (35)

$$\Phi(R) = \int\limits_0^R e^{-7\frac{H}{c}r} dr = \frac{c}{7H} \left(1 - e^{-7\frac{H}{c}R} \right), \tag{36}$$

and its graph is shown in Fig.4.

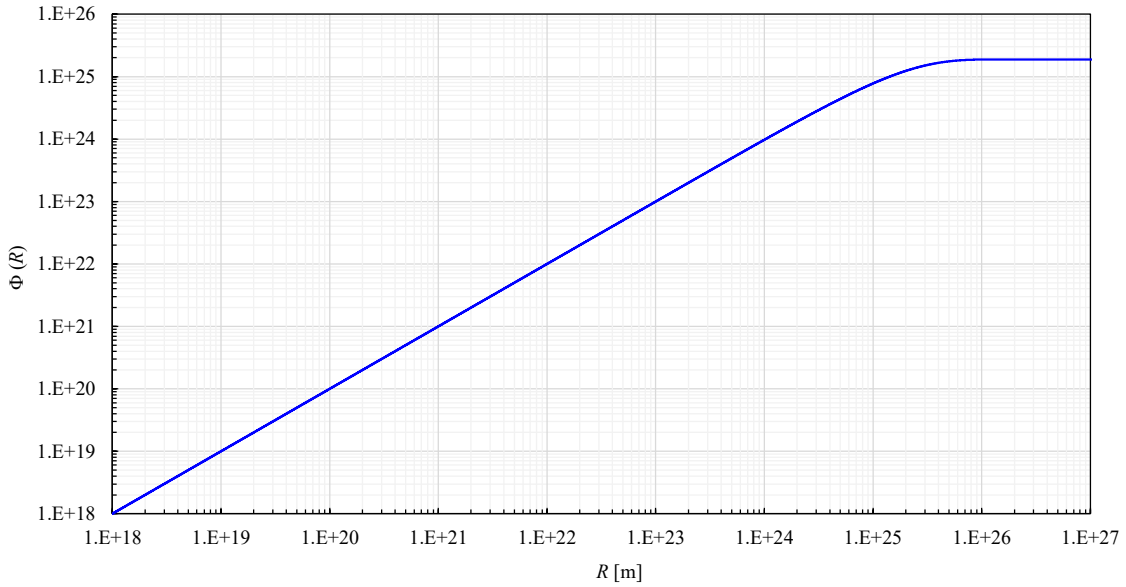

Fig.4 Dependence of the function $\Phi(R)$ (36) on the distance R of the observation sphere from the COP. The asymptotic plateau of the total intensity corresponds to a slightly smaller radius than predicted $R_{obs} \approx 4.3 \cdot 10^{26}$ m by the calculations of the standard model [30].

The asymptotic behaviour of the dependence (36) leads to the final value of the total intensity max I_Ω

$$\max I_\Omega(R) = \lim_{R\to\infty} I_\Omega(R) = 2n\sigma T(0)^4 \cdot \lim_{R\to\infty} \Phi(R) \to \boxed{\max I_\Omega(R) = 2n\sigma T(0)^4 \frac{c}{7H} \ll \infty}, \quad (37)$$

which is approximately reached already at distances of the order of $R \approx 10^{26}$ m, and the outer region contributes negligibly. This is how the problem of the Olbers' paradox is solved within the fully conformal metric.

While in a space with a standard Minkowski metric the radiation of all differential spheres would contribute equally to the total intensity at the COP, under the conditions of a conformal metric there is a kind of limit at which the differential contributions to the total intensity drop significantly to negligible values. This decrease can be expressed on the basis of relation (34) in the form of function

$$\Psi(r) = \frac{dI_\Omega(r)/dr}{dI_\Omega(0)/dr} = e^{-7\frac{H}{c}r}. \quad (38)$$

The dependence (38) is plotted in Fig. 5. The radial distance $r = 4 \cdot 10^{26}$ m from the COP, at which the intensity contribution drops by nine orders of magnitude to 1 ppb of the original value, agrees very well with the $R_{obs} \approx 4.3 \cdot 10^{26}$ m of the observable universe according to the standard model [30].

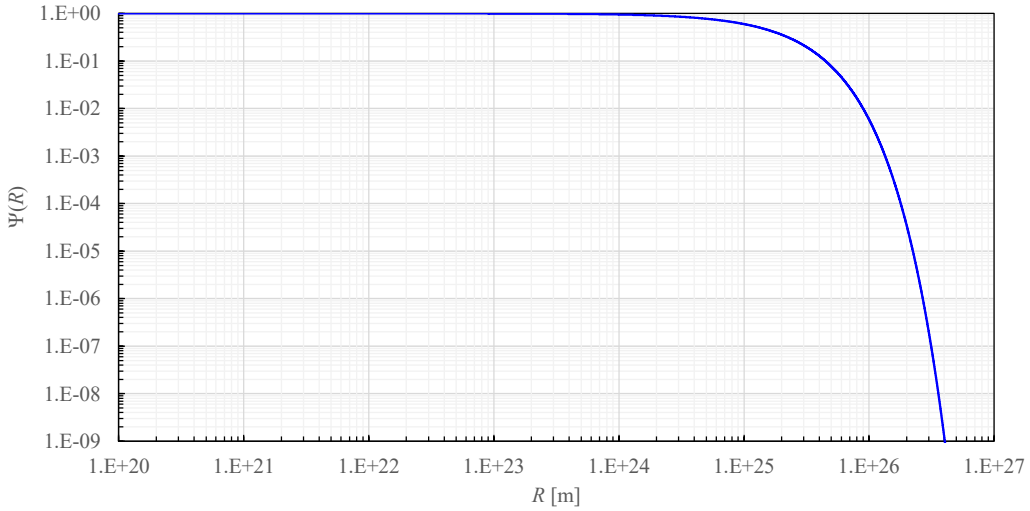

Fig.5 Dependence of the relative intensity decrease function $\Psi(R)$ (38) on the distance R from the COP.

The fully conformal metric thus defines a region of the observable universe where the contributions from the outer region are not zero in principle as in the case of causal cosmological horizon of the standard model, but they are completely negligible from an energy perspective. According to one of the most recent observations from the James Webb Telescope in 2022 [31], we can consider detecting objects with redshifts up to $z = 12$, which according to (20), corresponds to a distance of $3.5 \cdot 10^{26}$ m located the steep intensity drop of eight orders of magnitude in Fig. 5.

CONCLUSION

This contribution formulates and interprets a relatively simple global solution of Einstein's gravitational equations without the cosmological term and with a time-independent energy-momentum tensor. This solution takes the form of a fully conformal Minkowski metric which is globally scaled by the same time function $\psi(x_4)$ in all four space-time coordinates. The time-dependencies of the metric tensor $g_{\mu\nu}(x_4) = \psi(x_4)\eta_{\mu\nu}$ are fully compensated in the components of the Einstein tensor on the left-hand side of the gravitational equations with respect to the time-independent components of the energy-momentum tensor. Unlike the Robertson-Walker metric, the time independence of the speed of light is preserved in the above conformal metric. And similar to the rest mass, other local physical parameters, such as the electromagnetic spectrum and others, are conserved in the vicinity of an arbitrary COP. Under the conditions of the time-independence of the energy-momentum tensor, the clocks and gauges around all COPs must also be understood as identical, and the universe on a global scale as stationary. Changes in scales and rates of time flow observed over large distances (in the past) are only relative to a given COP, similar to the relativistic change in mass of moving particles. Given the universal nature of the local quantum definition of the time unit 1s, and the possibility of a natural choice of the origin of the COP ($x_4 = 0$) in the local presence of any observer, the exponential form of the scaling function $\psi(x_4)$ is covariant. All observers at rest with respect to the isotropic CMB field have their own local times, which flow at the same rate with respect to all local physical processes. However, the nonlinearity of the scaling function $\psi(x_4)$ has a real observable physical content and cannot be removed by formal time recalibration.

The experimental section then discusses some observational implications of this fully conformal metric. Without the need for a cosmological term in Einstein's gravitation equations, the above solution provides a generalised form and physical interpretation of the Hubble-Lemaître law $z(r) = (e^{Hr/c} - 1)$, which agrees very well with current astrophysical data even for very distant supernovae Ia. The whole concept of the model was motivated by considerations of whether cosmological redshifts can arise due to global metric differences, similar to the case of gravitational redshifts in the radiation emission of very massive objects.

The question of an alternative interpretation of the cosmological redshift was raised in the past by Fritz Zwicky. However, his concept of "tired light" corresponded to a gravitational redshift based on local curvatures of spacetime by the masses of galaxies, and the redshift effect depended on local spatial distances from galactic centres. This created a problem with observational data showing a global dependence of redshift on distance from any observer.

On cosmological scales, the global conformal solution also shows interesting agreement with experimental observations of the spatial distribution of real astrophysical sources such as γ-ray bursts and quasars. The conformal metric field model also solves in principle the problem of the critical global density, the flatness of 3D space and Olbers' paradox. The strict principle of a sharp cosmological horizon in the Standard Model is replaced in the case of the conformal metric by a much softer formulation - a region of the practically observable universe that does not represent sharp causal horizon.

This paper should not be seen as a confrontation with the established standard cosmological model, but as a methodological attempt to describe and possibly explain the real observed spacetime distribution of some astrophysical sources. The next upcoming work is focused on the generalization of the Schwartschild solution on the background of the above mentioned fully conformal metric and derivation of the corresponding state equation.

ACKNOWLEDGEMENT

The work was supported by the project No. CZ.02.01.01/00/22_008/0004631. Materials and technologies for sustainable development within the Jan Amos Komensky Operational Program financed by the European Union and from the state budget of the Czech Republic and the European Union under the REFRESH – Research Excellence For Region Sustainability and High-tech Industries project number CZ.10.03.01/00/22_003/0000048 via the Operational Programme Just Transition. I thank, to my colleague Jiri Bednar for his careful review and preparation of the English text and first and foremost I am very grateful to Jeyninka for great support in my work.

DATA AVAILABILITY

NASA (1996) Gamma-Ray Astrophysics: NSSTC, BATSE4B, CMAXMIN TABLE
Available at: https://gammaray.nsstc.nasa.gov/batse/grb/catalog/4b/4br_cmax_cmin.html.
NASA (2022) NASA/IPAC EXTRAGALACTIC DATABASE (2022): Date and Time of the Query: Sun Nov 12 09:25:30 2017PDT
Available at: https://ned.ipac.caltech.edu/.
Planck 2013 (2013) Planck 2013 results.: I. Overview of products and scientific results, Astronomy & Astrophysics manuscript no. Planck Mission
Available at: https://arxiv.org/pdf/1303.5062.pdf.

LITERATURE

[1] F. Zwicky, "ON THE REDSHIFT OF SPECTRAL LINES THROUGH INTERSTELLAR SPACE," *Proc. Natl. Acad. Sci.*, vol. 15, no. 10, pp. 773–779, Oct. 1929, doi: 10.1073/pnas.15.10.773.

[2] H. Bondi and T. Gold, "The Steady-State Theory of the Expanding Universe," *Mon. Not. R. Astron. Soc.*, vol. 108, no. 3, pp. 252–270, Jun. 1948, doi: 10.1093/mnras/108.3.252.

[3] F. Hoyle, "A New Model for the Expanding Universe," *Mon. Not. R. Astron. Soc.*, vol. 108, no. 5, pp. 372–382, Oct. 1948, doi: 10.1093/mnras/108.5.372.

[4] J. D. Bekenstein, "Exact solutions of Einstein-conformal scalar equations," *Ann. Phys. (N. Y).*, vol. 82, no. 2, 1974, doi: 10.1016/0003-4916(74)90124-9.

[5] J. A. Lester, "Conformal Minkowski space-time - I. - Relative infinity and proper time," *Nuovo Cim. B*, vol. 72, no. 2, 1982, doi: 10.1007/BF02829408.

[6] J. A. Lester, "Conformal Minkowski spacetime - II - A Cosmological model," *Nuovo Cim B*, pp. 139–149, 1983.

[7] G. U. Varieschi, "A kinematical approach to conformal cosmology," *Gen. Relativ. Gravit.*, vol. 42, no. 4, 2010, doi: 10.1007/s10714-009-0890-y.

[8] D. Behnke, D. B. Blaschke, V. N. Pervushin, and D. Proskurin, "Description of supernova data in conformal cosmology without cosmological constant," *Phys. Lett. Sect. B Nucl. Elem. Part. High-Energy Phys.*, vol. 530, no. 1–4, 2002, doi: 10.1016/S0370-2693(02)01341-2.

[9] M. Libanov, V. Rubakov, and G. Rubtsov, "Towards conformal cosmology," *JETP Lett.*, vol. 102, no. 8, 2015, doi: 10.1134/S0021364015200072.

[10] M. M. Kumar, "Some significant conformal metrics," *Nuovo Cim. A Ser. 10*, vol. 63, no. 2, 1969, doi: 10.1007/BF02756233.

[11] A. G. Lematre, "A Homogeneous Universe of Constant Mass and Increasing Radius accounting for the Radial Velocity of Extra-galactic Nebulae," *Mon. Not. R. Astron. Soc.*, vol. 91, no. 5, pp. 483–490, Mar. 1931, doi: 10.1093/mnras/91.5.483.

[12] A. Friedmann, "On the Possibility of a World with Constant Negative Curvature of Space," *Gen. Relativ. Gravit.*, vol. 31, no. 12, pp. 2001–2008, Dec. 1999, doi: 10.1023/A:1026755309811.

[13] H. P. Robertson, "Kinematics and World-Structure," *Astrophys. J.*, vol. 82, p. 284, Nov. 1935, doi: 10.1086/143681.

[14] A. G. Walker, "On Milne's Theory of World-Structure *," *Proc. London Math. Soc.*, vol. s2-42, no. 1, pp. 90–127, 1937, doi: 10.1112/plms/s2-42.1.90.

[15] Weinberg S, *Relativity, gravitation and Cosmology*. John Wiley & Sons Inc. , 1972.

[16] M. Ibison, "On the conformal forms of the Robertson-Walker metric," *J. Math. Phys.*, vol. 48, no. 12, 2007, doi: 10.1063/1.2815811.

[17] C. W. Misner, K. S. Thorne, and J. A. Wheeler, "MTW-Gravitation," in *Gravitation*, 2018.

[18] P. J. . Peebles, *Principles of Physical Cosmology*. 2020. doi: 10.2307/j.ctvxrpxvb.

[19] Kuchař K, *Fundamentals of general relativity*. Prahy: ACADEMIA , 1968.

[20] Weinberg S, *Cosmology*. Oxford Press , 2008.

[21] NASA, "NASA/IPAC EXTRAGALACTIC DATABASE (2022): Date and Time of the Query: Sun Nov

12 09:25:30 2017PDT," *https://ned.ipac.caltech.edu/*, 2022.

[22] Planck 2013, "Planck 2013 results.: I. Overview of products and scientific results, Astronomy & Astrophysics manuscript no. Planck Mission," *https://arxiv.org/pdf/1303.5062.pdf*, 2013.

[23] M. Schmidt, J. C. Higdon, and G. Hueter, "Application of the V/V(max) test to gamma-ray bursts," *Astrophys. J.*, vol. 329, 1988, doi: 10.1086/185182.

[24] D. L. Band, "The effect of repeating burst sources on ⟨V/Vmax⟩," in *AIP Conference Proceedings*, 1994, vol. 307, pp. 39–43. doi: 10.1063/1.45902.

[25] C. A. Meegan *et al.*, "Spatial distribution of γ-ray bursts observed by BATSE," *Nature*, vol. 355, no. 6356, 1992, doi: 10.1038/355143a0.

[26] NASA, "Gamma-Ray Astrophysics: NSSTC, BATSE4B, CMAXMIN TABLE ," *https://gammaray.nsstc.nasa.gov/batse/grb/catalog/4b/4br_cmax_cmin.html*, 1996. https://gammaray.nsstc.nasa.gov/batse/grb/catalog/4b/4br_cmax_cmin.html (accessed Feb. 23, 2023).

[27] O. S. Salafia and G. Ghirlanda, "The Structure of Gamma Ray Burst Jets," *Galaxies*, vol. 10, no. 5, p. 93, Aug. 2022, doi: 10.3390/galaxies10050093.

[28] D. W. Sciama and M. J. Rees, "Cosmological significance of the relation between red-shift and flux density for quasars [1]," *Nature*, vol. 211, no. 5055. 1966. doi: 10.1038/2111283a0.

[29] MILLIQUAS v7.9, "MILLIQUAS v7.9: Quasars, Redshifts and the 'accelerating-expansion' Universe.Data, sky fields, & some thoughts on the right Cosmological model," *http://quasars.org/milliquas.htm* , 2021.

[30] Halpern P and Tomasello N, "Size of the Observable Universe," *Adv. Astrophys.*, vol. 1, no. 3, 2016.

[31] Finkelstein S et al, "A Long Time Ago in a Galaxy Far, Far Away: A Candidate z∼12 Galaxy in Early JWST CEERS Imaging," *Astrophys. J. Lett.*, vol. 940:L55, 2022.

APPENDIX 1.

M4 - space

$$\Gamma^{\mu}{}_{\nu\lambda} = \frac{1}{2} g^{\mu\alpha}\left(\partial_\nu g_{\alpha\lambda} + \partial_\lambda g_{\alpha\nu} - \partial_\alpha g_{\nu\lambda}\right)$$

$$\boxed{\Gamma^{\mu}{}_{\nu\lambda} = \frac{1}{2} g^{\mu 1}\left(\partial_\nu g_{1\lambda} + \partial_\lambda g_{1\nu}\right) + \frac{1}{2} g^{\mu 2}\left(\partial_\nu g_{2\lambda} + \partial_\lambda g_{2\nu}\right) + \frac{1}{2} g^{\mu 3}\left(\partial_\nu g_{3\lambda} + \partial_\lambda g_{3\nu}\right) + \frac{1}{2} g^{\mu 4}\left(\partial_\nu g_{4\lambda} + \partial_\lambda g_{4\nu} - \partial_4 g_{\nu\lambda}\right)}$$

$$\begin{aligned}
g_{11}(x_4) &= \psi(x_4)\eta_{11} = \psi(x_4)\\
g_{22}(x_4) &= \psi(x_4)\eta_{22} = \psi(x_4)\\
g_{33}(x_4) &= \psi(x_4)\eta_{33} = \psi(x_4)\\
g_{44}(x_4) &= \psi(x_4)\eta_{44} = -\psi(x_4)
\end{aligned}$$

$$\Gamma^{1}{}_{\nu\lambda} = \frac{1}{2} g^{11}\left(\partial_\nu g_{1\lambda} + \partial_\lambda g_{1\nu}\right) \rightarrow \begin{cases}
\Gamma^{1}{}_{1\lambda} = \frac{1}{2} g^{11}\left(\underbrace{\partial_1 g_{1\lambda}}_{0} + \partial_\lambda g_{11}\right) = \frac{1}{2} g^{11}\partial_\lambda g_{11} \rightarrow \boxed{\Gamma^{1}{}_{14} = \frac{1}{2} g^{11}\partial_4 g_{11} \rightarrow \Gamma^{1}{}_{14} = \frac{1}{2}\psi(x_4)^{-1}\partial_4\psi(x_4)}\\
\Gamma^{1}{}_{2\lambda} = \frac{1}{2} g^{11}\left(\underbrace{\partial_2 g_{1\lambda}}_{0} + \partial_\lambda \underbrace{g_{12}}_{0}\right) = 0\\
\Gamma^{1}{}_{3\lambda} = \frac{1}{2} g^{11}\left(\underbrace{\partial_3 g_{1\lambda}}_{0} + \partial_\lambda \underbrace{g_{13}}_{0}\right) = 0\\
\Gamma^{1}{}_{4\lambda} = \frac{1}{2} g^{11}\left(\partial_4 g_{1\lambda} + \partial_\lambda \underbrace{g_{14}}_{0}\right) = \frac{1}{2} g^{11}\partial_4 g_{1\lambda} \rightarrow \boxed{\Gamma^{1}{}_{41} = \frac{1}{2} g^{11}\partial_4 g_{11} \rightarrow \Gamma^{1}{}_{41} = \frac{1}{2}\psi(x_4)^{-1}\partial_4\psi(x_4)}
\end{cases}$$

$$\Gamma^{2}{}_{\nu\lambda} = \frac{1}{2} g^{22}\left(\partial_\nu g_{2\lambda} + \partial_\lambda g_{2\nu}\right) \rightarrow \begin{cases}
\Gamma^{2}{}_{1\lambda} = \frac{1}{2} g^{22}\left(\underbrace{\partial_1 g_{2\lambda}}_{0} + \partial_\lambda \underbrace{g_{21}}_{0}\right) = 0\\
\Gamma^{2}{}_{2\lambda} = \frac{1}{2} g^{22}\left(\underbrace{\partial_2 g_{2\lambda}}_{0} + \partial_\lambda g_{22}\right) = \frac{1}{2} g^{22}\partial_\lambda g_{22} \rightarrow \boxed{\Gamma^{2}{}_{24} = \frac{1}{2} g^{22}\partial_4 g_{22} \rightarrow \Gamma^{2}{}_{24} = \frac{1}{2}\psi(x_4)^{-1}\partial_4\psi(x_4)}\\
\Gamma^{2}{}_{3\lambda} = \frac{1}{2} g^{22}\left(\underbrace{\partial_3 g_{2\lambda}}_{0} + \partial_\lambda \underbrace{g_{23}}_{0}\right) = 0\\
\Gamma^{2}{}_{4\lambda} = \frac{1}{2} g^{22}\left(\partial_4 g_{2\lambda} + \partial_\lambda \underbrace{g_{24}}_{0}\right) = \frac{1}{2} g^{22}\partial_4 g_{2\lambda} \rightarrow \boxed{\Gamma^{2}{}_{42} = \frac{1}{2} g^{22}\partial_4 g_{22} \rightarrow \Gamma^{2}{}_{42} = \frac{1}{2}\psi(x_4)^{-1}\partial_4\psi(x_4)}
\end{cases}$$

$$\Gamma^{3}{}_{\nu\lambda} = \frac{1}{2} g^{33}\left(\partial_\nu g_{3\lambda} + \partial_\lambda g_{3\nu}\right) \rightarrow \begin{cases}
\Gamma^{3}{}_{1\lambda} = \frac{1}{2} g^{33}\left(\underbrace{\partial_1 g_{3\lambda}}_{0} + \partial_\lambda \underbrace{g_{31}}_{0}\right) = 0\\
\Gamma^{3}{}_{2\lambda} = \frac{1}{2} g^{33}\left(\underbrace{\partial_2 g_{3\lambda}}_{0} + \partial_\lambda \underbrace{g_{32}}_{0}\right) = 0\\
\Gamma^{3}{}_{3\lambda} = \frac{1}{2} g^{33}\left(\underbrace{\partial_3 g_{3\lambda}}_{0} + \partial_\lambda g_{33}\right) = \frac{1}{2} g^{33}\partial_\lambda g_{33} \rightarrow \boxed{\Gamma^{3}{}_{34} = \frac{1}{2} g^{33}\partial_4 g_{33} \rightarrow \Gamma^{3}{}_{34} = \frac{1}{2}\psi(x_4)^{-1}\partial_4\psi(x_4)}\\
\Gamma^{3}{}_{4\lambda} = \frac{1}{2} g^{33}\left(\partial_4 g_{3\lambda} + \partial_\lambda \underbrace{g_{34}}_{0}\right) = \frac{1}{2} g^{33}\partial_4 g_{3\lambda} \rightarrow \boxed{\Gamma^{3}{}_{43} = \frac{1}{2} g^{33}\partial_4 g_{33} \rightarrow \Gamma^{3}{}_{43} = \frac{1}{2}\psi(x_4)^{-1}\partial_4\psi(x_4)}
\end{cases}$$

$$\Gamma^{4}{}_{\nu\lambda} = \frac{1}{2} g^{44}\left(\partial_\nu g_{4\lambda} + \partial_\lambda g_{4\nu} - \partial_4 g_{\nu\lambda}\right) \rightarrow \begin{cases}
\Gamma^{4}{}_{1\lambda} = \frac{1}{2} g^{44}\left(\underbrace{\partial_1 g_{4\lambda}}_{0} + \partial_\lambda \underbrace{g_{41}}_{0} - \partial_4 g_{1\lambda}\right) = -\frac{1}{2} g^{44}\partial_4 g_{1\lambda} \rightarrow \boxed{\begin{aligned}\Gamma^{4}{}_{11} &= -\frac{1}{2} g^{44}\partial_4 g_{11} \rightarrow\\ \Gamma^{4}{}_{11} &= \frac{1}{2}\psi(x_4)^{-1}\partial_4\psi(x_4)\end{aligned}}\\
\Gamma^{4}{}_{2\lambda} = \frac{1}{2} g^{44}\left(\underbrace{\partial_2 g_{4\lambda}}_{0} + \partial_\lambda \underbrace{g_{42}}_{0} - \partial_4 g_{2\lambda}\right) = -\frac{1}{2} g^{44}\partial_4 g_{2\lambda} \rightarrow \boxed{\begin{aligned}\Gamma^{4}{}_{22} &= -\frac{1}{2} g^{44}\partial_4 g_{22} \rightarrow\\ \Gamma^{4}{}_{22} &= \frac{1}{2}\psi(x_4)^{-1}\partial_4\psi(x_4)\end{aligned}}\\
\Gamma^{4}{}_{3\lambda} = \frac{1}{2} g^{44}\left(\underbrace{\partial_3 g_{4\lambda}}_{0} + \partial_\lambda \underbrace{g_{43}}_{0} - \partial_4 g_{3\lambda}\right) = -\frac{1}{2} g^{44}\partial_4 g_{3\lambda} \rightarrow \boxed{\begin{aligned}\Gamma^{4}{}_{33} &= -\frac{1}{2} g^{44}\partial_4 g_{33} \rightarrow\\ \Gamma^{4}{}_{33} &= \frac{1}{2}\psi(x_4)^{-1}\partial_4\psi(x_4)\end{aligned}}\\
\Gamma^{4}{}_{4\lambda} = \frac{1}{2} g^{44}\left(\partial_4 g_{4\lambda} + \partial_\lambda g_{44} - \partial_4 g_{4\lambda}\right) \rightarrow \boxed{\Gamma^{4}{}_{44} = \frac{1}{2} g^{44}\partial_4 g_{44} \rightarrow \Gamma^{4}{}_{44} = \frac{1}{2}\psi(x_4)^{-1}\partial_4\psi(x_4)}
\end{cases}$$

APPENDIX 2.

E3 - space

$$\Gamma^{\mu}{}_{\nu\lambda} = \tfrac{1}{2} g^{\mu\alpha}\left(\partial_{\nu} g_{\alpha\lambda} + \partial_{\lambda} g_{\alpha\nu} - \partial_{\alpha} g_{\nu\lambda}\right)$$

$$\boxed{\Gamma^{\mu}{}_{\nu\lambda} = \frac{1}{2} g^{\mu 1}\left(\partial_{\nu} g_{1\lambda} + \partial_{\lambda} g_{1\nu}\right) + \frac{1}{2} g^{\mu 2}\left(\partial_{\nu} g_{2\lambda} + \partial_{\lambda} g_{2\nu}\right) + \frac{1}{2} g^{\mu 3}\left(\partial_{\nu} g_{3\lambda} + \partial_{\lambda} g_{3\nu}\right)}$$

$$\Gamma^{1}{}_{\nu\lambda} = \frac{1}{2} g^{11}\left(\partial_{\nu} g_{1\lambda} + \partial_{\lambda} g_{1\nu}\right) \rightarrow \begin{cases} \Gamma^{1}{}_{1\lambda} = \frac{1}{2} g^{11}\left(\underbrace{\partial_{1} g_{1\lambda}}_{0} + \partial_{\lambda} g_{11}\right) = \frac{1}{2} g^{11} \partial_{\lambda} g_{11} = 0 \\ \Gamma^{1}{}_{2\lambda} = \frac{1}{2} g^{11}\left(\underbrace{\partial_{2} g_{1\lambda}}_{0} + \partial_{\lambda} \underbrace{g_{12}}_{0}\right) = 0 \\ \Gamma^{1}{}_{3\lambda} = \frac{1}{2} g^{11}\left(\underbrace{\partial_{3} g_{1\lambda}}_{0} + \partial_{\lambda} \underbrace{g_{13}}_{0}\right) = 0 \end{cases}$$

$$\Gamma^{2}{}_{\nu\lambda} = \frac{1}{2} g^{22}\left(\partial_{\nu} g_{2\lambda} + \partial_{\lambda} g_{2\nu}\right) \rightarrow \begin{cases} \Gamma^{2}{}_{1\lambda} = \frac{1}{2} g^{22}\left(\underbrace{\partial_{1} g_{2\lambda}}_{0} + \partial_{\lambda} \underbrace{g_{21}}_{0}\right) = 0 \\ \Gamma^{2}{}_{2\lambda} = \frac{1}{2} g^{22}\left(\underbrace{\partial_{2} g_{2\lambda}}_{0} + \partial_{\lambda} g_{22}\right) = \frac{1}{2} g^{22} \partial_{\lambda} g_{22} = 0 \\ \Gamma^{2}{}_{3\lambda} = \frac{1}{2} g^{22}\left(\underbrace{\partial_{3} g_{2\lambda}}_{0} + \partial_{\lambda} \underbrace{g_{23}}_{0}\right) = 0 \end{cases}$$

$$\Gamma^{3}{}_{\nu\lambda} = \frac{1}{2} g^{33}\left(\partial_{\nu} g_{3\lambda} + \partial_{\lambda} g_{3\nu}\right) \rightarrow \begin{cases} \Gamma^{3}{}_{1\lambda} = \frac{1}{2} g^{33}\left(\underbrace{\partial_{1} g_{3\lambda}}_{0} + \partial_{\lambda} \underbrace{g_{31}}_{0}\right) = 0 \\ \Gamma^{3}{}_{2\lambda} = \frac{1}{2} g^{33}\left(\underbrace{\partial_{2} g_{3\lambda}}_{0} + \partial_{\lambda} \underbrace{g_{32}}_{0}\right) = 0 \\ \Gamma^{3}{}_{3\lambda} = \frac{1}{2} g^{33}\left(\underbrace{\partial_{3} g_{3\lambda}}_{0} + \partial_{\lambda} g_{33}\right) = \frac{1}{2} g^{33} \partial_{\lambda} g_{33} = 0 \end{cases}$$

APPENDIX 3.

M4 - space

$$R_{\lambda\nu} = \partial_{\mu}\Gamma^{\mu}{}_{\nu\lambda} - \partial_{\nu}\Gamma^{\mu}{}_{\mu\lambda} + \Gamma^{\eta}{}_{\nu\lambda}\Gamma^{\mu}{}_{\mu\eta} - \Gamma^{\eta}{}_{\mu\lambda}\Gamma^{\mu}{}_{\nu\eta} \rightarrow \begin{cases} R_{11} = \partial_4\Gamma^4{}_{11} + \Gamma^{\eta}{}_{11}\Gamma^{\mu}{}_{\mu\eta} - \Gamma^{\eta}{}_{\mu 1}\Gamma^{\mu}{}_{1\eta} \\ R_{22} = \partial_4\Gamma^4{}_{22} + \Gamma^{\eta}{}_{22}\Gamma^{\mu}{}_{\mu\eta} - \Gamma^{\eta}{}_{\mu 2}\Gamma^{\mu}{}_{2\eta} \\ R_{33} = \partial_4\Gamma^4{}_{33} + \Gamma^{\eta}{}_{33}\Gamma^{\mu}{}_{\mu\eta} - \Gamma^{\eta}{}_{\mu 3}\Gamma^{\mu}{}_{3\eta} \\ R_{44} = \partial_4\Gamma^4{}_{44} - \partial_4\Gamma^{\mu}{}_{\mu 4} + \Gamma^{\eta}{}_{44}\Gamma^{\mu}{}_{\mu\eta} - \Gamma^{\eta}{}_{\mu 4}\Gamma^{\mu}{}_{4\eta} \end{cases}$$

$$\boxed{R_{11} = \boxed{\partial_1\Gamma^1{}_{11} + \partial_2\Gamma^2{}_{11} + \partial_3\Gamma^3{}_{11}} + \partial_4\Gamma^4{}_{11} + \Gamma^{\eta}{}_{11}\Gamma^{\mu}{}_{\mu\eta} - \Gamma^{\eta}{}_{\mu 1}\Gamma^{\mu}{}_{1\eta}}$$

$$R_{11} = \partial_4\Gamma^4{}_{11} + \begin{bmatrix} \left(\Gamma^1{}_{11}\Gamma^1{}_{11} - \Gamma^1{}_{11}\Gamma^1{}_{11}\right) + \left(\Gamma^1{}_{11}\Gamma^2{}_{21} - \Gamma^1{}_{21}\Gamma^2{}_{11}\right) + \left(\Gamma^1{}_{11}\Gamma^3{}_{31} - \Gamma^1{}_{31}\Gamma^3{}_{11}\right) + \left(\Gamma^1{}_{11}\Gamma^4{}_{41} - \Gamma^1{}_{41}\Gamma^4{}_{11}\right) \\ + \left(\Gamma^2{}_{11}\Gamma^1{}_{12} - \Gamma^2{}_{11}\Gamma^1{}_{12}\right) + \left(\Gamma^2{}_{11}\Gamma^2{}_{22} - \Gamma^2{}_{21}\Gamma^2{}_{12}\right) + \left(\Gamma^2{}_{11}\Gamma^3{}_{32} - \Gamma^2{}_{31}\Gamma^3{}_{12}\right) + \left(\Gamma^2{}_{11}\Gamma^4{}_{42} - \Gamma^2{}_{41}\Gamma^4{}_{12}\right) \\ + \left(\Gamma^3{}_{11}\Gamma^1{}_{13} - \Gamma^3{}_{11}\Gamma^1{}_{13}\right) + \left(\Gamma^3{}_{11}\Gamma^2{}_{23} - \Gamma^3{}_{21}\Gamma^2{}_{13}\right) + \left(\Gamma^3{}_{11}\Gamma^3{}_{33} - \Gamma^3{}_{31}\Gamma^3{}_{13}\right) + \left(\Gamma^3{}_{11}\Gamma^4{}_{43} - \Gamma^3{}_{41}\Gamma^4{}_{13}\right) \\ + \left(\Gamma^4{}_{11}\Gamma^1{}_{14} - \Gamma^4{}_{11}\Gamma^1{}_{14}\right) + \left(\Gamma^4{}_{11}\Gamma^2{}_{24} - \Gamma^4{}_{21}\Gamma^2{}_{14}\right) + \left(\Gamma^4{}_{11}\Gamma^3{}_{34} - \Gamma^4{}_{31}\Gamma^3{}_{14}\right) + \left(\Gamma^4{}_{11}\Gamma^4{}_{44} - \Gamma^4{}_{41}\Gamma^4{}_{14}\right) \end{bmatrix}$$

$$R_{11} = \partial_4\Gamma^4{}_{11} + \begin{bmatrix} \left(\boxed{\Gamma^1{}_{11}\Gamma^1{}_{11} - \Gamma^1{}_{11}\Gamma^1{}_{11}}\right) + \left(\boxed{\Gamma^1{}_{11}}\Gamma^2{}_{21} - \boxed{\Gamma^1{}_{21}}\Gamma^2{}_{11}\right) + \left(\boxed{\Gamma^1{}_{11}}\Gamma^3{}_{31} - \boxed{\Gamma^1{}_{31}}\Gamma^3{}_{11}\right) + \left(\boxed{\Gamma^1{}_{11}}\Gamma^4{}_{41} - \Gamma^1{}_{41}\Gamma^4{}_{11}\right) \\ + \left(\boxed{\Gamma^2{}_{11}\Gamma^1{}_{12} - \Gamma^2{}_{11}\Gamma^1{}_{12}}\right) + \left(\boxed{\Gamma^2{}_{11}}\Gamma^2{}_{22} - \boxed{\Gamma^2{}_{21}}\Gamma^2{}_{12}\right) + \left(\boxed{\Gamma^2{}_{11}}\Gamma^3{}_{32} - \boxed{\Gamma^2{}_{31}}\Gamma^3{}_{12}\right) + \left(\boxed{\Gamma^2{}_{11}}\Gamma^4{}_{42} - \boxed{\Gamma^2{}_{41}}\Gamma^4{}_{12}\right) \\ + \left(\boxed{\Gamma^3{}_{11}\Gamma^1{}_{13} - \Gamma^3{}_{11}\Gamma^1{}_{13}}\right) + \left(\boxed{\Gamma^3{}_{11}}\Gamma^2{}_{23} - \boxed{\Gamma^3{}_{21}}\Gamma^2{}_{13}\right) + \left(\boxed{\Gamma^3{}_{11}}\Gamma^3{}_{33} - \boxed{\Gamma^3{}_{31}}\Gamma^3{}_{13}\right) + \left(\boxed{\Gamma^3{}_{11}}\Gamma^4{}_{43} - \boxed{\Gamma^3{}_{41}}\Gamma^4{}_{13}\right) \\ + \left(\boxed{\Gamma^4{}_{11}\Gamma^1{}_{14} - \Gamma^4{}_{11}\Gamma^1{}_{14}}\right) + \left(\Gamma^4{}_{11}\Gamma^2{}_{24} - \boxed{\Gamma^4{}_{21}}\Gamma^2{}_{14}\right) + \left(\Gamma^4{}_{11}\Gamma^3{}_{34} - \boxed{\Gamma^4{}_{31}}\Gamma^3{}_{14}\right) + \left(\Gamma^4{}_{11}\Gamma^4{}_{44} - \boxed{\Gamma^4{}_{41}}\Gamma^4{}_{14}\right) \end{bmatrix}$$

$$R_{11} = \partial_4\Gamma^4{}_{11} + \left[\left(-\Gamma^1{}_{41}\Gamma^4{}_{11}\right) + \left(\Gamma^4{}_{11}\Gamma^2{}_{24}\right) + \left(\Gamma^4{}_{11}\Gamma^3{}_{34}\right) + \left(\Gamma^4{}_{11}\Gamma^4{}_{44}\right)\right]$$

$$R_{11} = \partial_4\left(\frac{1}{2}\partial_4\ln\psi(x_4)\right) + \left[-\left(\frac{1}{2}\partial_4\ln\psi(x_4)\right)^2 + \left(\frac{1}{2}\partial_4\ln\psi(x_4)\right)^2 + \left(\frac{1}{2}\partial_4\ln\psi(x_4)\right)^2 + \left(\frac{1}{2}\partial_4\ln\psi(x_4)\right)^2\right]$$

$$\boxed{R_{11} = \frac{1}{2}\partial_4{}^2\ln\psi(x_4) + \frac{1}{2}\left(\partial_4\ln\psi(x_4)\right)^2}$$

$$\boxed{R_{22} = \partial_4\Gamma^4{}_{22} + \Gamma^{\eta}{}_{22}\Gamma^{\mu}{}_{\mu\eta} - \Gamma^{\eta}{}_{\mu 2}\Gamma^{\mu}{}_{2\eta}}$$

$$R_{22} = \partial_4\Gamma^4{}_{22} + \Gamma^{\eta}{}_{22}\Gamma^{\mu}{}_{\mu\eta} - \Gamma^{\eta}{}_{\mu 2}\Gamma^{\mu}{}_{2\eta}$$

$$\boxed{R_{22} = \frac{1}{2}\partial_4{}^2\ln\psi(x_4) + \frac{1}{2}\left(\partial_4\ln\psi(x_4)\right)^2}$$

$$\boxed{R_{33} = \partial_4\Gamma^4{}_{33} + \Gamma^{\eta}{}_{33}\Gamma^{\mu}{}_{\mu\eta} - \Gamma^{\eta}{}_{\mu 3}\Gamma^{\mu}{}_{3\eta}}$$

$$R_{33} = \partial_4\Gamma^4{}_{33} + \Gamma^{\eta}{}_{33}\Gamma^{\mu}{}_{\mu\eta} - \Gamma^{\eta}{}_{\mu 3}\Gamma^{\mu}{}_{3\eta}$$

$$\boxed{R_{33} = \frac{1}{2}\partial_4{}^2\ln\psi(x_4) + \frac{1}{2}\left(\partial_4\ln\psi(x_4)\right)^2}$$

$$\left(\Gamma^1{}_{14} = \Gamma^1{}_{41}\right) = \left(\Gamma^2{}_{24} = \Gamma^2{}_{42}\right) = \left(\Gamma^3{}_{34} = \Gamma^3{}_{43}\right) = \left(\Gamma^4{}_{11} = \Gamma^4{}_{22} = \Gamma^4{}_{33} = \Gamma^4{}_{44}\right) = \frac{1}{2}\partial_4\ln\psi(x_4)$$

$$\boxed{R_{44} = \boxed{\partial_1\Gamma^1{}_{11} + \partial_2\Gamma^2{}_{11} + \partial_3\Gamma^3{}_{11}} + \partial_4\Gamma^4{}_{11} - \partial_4\Gamma^{\mu}{}_{\mu 4} + \Gamma^{\eta}{}_{44}\Gamma^{\mu}{}_{\mu\eta} - \Gamma^{\eta}{}_{\mu 4}\Gamma^{\mu}{}_{4\eta}}$$

$$R_{44} = \partial_4\Gamma^4{}_{44} - \left[\partial_4\Gamma^1{}_{14} + \partial_4\Gamma^2{}_{24} + \partial_4\Gamma^3{}_{34} + \partial_4\Gamma^4{}_{44}\right]$$
$$+ \begin{bmatrix} \left(\Gamma^1{}_{44}\Gamma^1{}_{11} - \Gamma^1{}_{14}\Gamma^1{}_{41}\right) + \left(\Gamma^1{}_{44}\Gamma^2{}_{21} - \Gamma^1{}_{24}\Gamma^2{}_{41}\right) + \left(\Gamma^1{}_{44}\Gamma^3{}_{31} - \Gamma^1{}_{34}\Gamma^3{}_{41}\right) + \left(\Gamma^1{}_{44}\Gamma^4{}_{41} - \Gamma^1{}_{44}\Gamma^4{}_{41}\right) \\ + \left(\Gamma^2{}_{44}\Gamma^1{}_{12} - \Gamma^2{}_{14}\Gamma^1{}_{42}\right) + \left(\Gamma^2{}_{44}\Gamma^2{}_{22} - \Gamma^2{}_{24}\Gamma^2{}_{42}\right) + \left(\Gamma^2{}_{44}\Gamma^3{}_{32} - \Gamma^2{}_{34}\Gamma^3{}_{42}\right) + \left(\Gamma^2{}_{44}\Gamma^4{}_{42} - \Gamma^2{}_{44}\Gamma^4{}_{42}\right) \\ + \left(\Gamma^3{}_{44}\Gamma^1{}_{13} - \Gamma^3{}_{14}\Gamma^1{}_{43}\right) + \left(\Gamma^3{}_{44}\Gamma^2{}_{23} - \Gamma^3{}_{24}\Gamma^2{}_{43}\right) + \left(\Gamma^3{}_{44}\Gamma^3{}_{33} - \Gamma^3{}_{34}\Gamma^3{}_{43}\right) + \left(\Gamma^3{}_{44}\Gamma^4{}_{43} - \Gamma^3{}_{44}\Gamma^4{}_{43}\right) \\ + \left(\Gamma^4{}_{44}\Gamma^1{}_{14} - \Gamma^4{}_{14}\Gamma^1{}_{44}\right) + \left(\Gamma^4{}_{44}\Gamma^2{}_{24} - \Gamma^4{}_{24}\Gamma^2{}_{44}\right) + \left(\Gamma^4{}_{44}\Gamma^3{}_{34} - \Gamma^4{}_{34}\Gamma^3{}_{44}\right) + \left(\Gamma^4{}_{44}\Gamma^4{}_{44} - \Gamma^4{}_{44}\Gamma^4{}_{44}\right) \end{bmatrix}$$

$$R_{44} = \partial_4\Gamma^4{}_{44} - \left[\partial_4\Gamma^1{}_{14} + \partial_4\Gamma^2{}_{24} + \partial_4\Gamma^3{}_{34} + \partial_4\Gamma^4{}_{44}\right]$$
$$+ \begin{bmatrix} \left(\boxed{\Gamma^1{}_{44}}\Gamma^1{}_{11} - \Gamma^1{}_{14}\Gamma^1{}_{41}\right) + \left(\boxed{\Gamma^1{}_{44}}\Gamma^2{}_{21} - \boxed{\Gamma^1{}_{24}}\Gamma^2{}_{41}\right) + \left(\boxed{\Gamma^1{}_{44}}\Gamma^3{}_{31} - \boxed{\Gamma^1{}_{34}}\Gamma^3{}_{41}\right) + \left(\boxed{\Gamma^1{}_{44}}\Gamma^4{}_{41} - \boxed{\Gamma^1{}_{44}}\Gamma^4{}_{41}\right) \\ + \left(\boxed{\Gamma^2{}_{44}}\Gamma^1{}_{12} - \boxed{\Gamma^2{}_{14}}\Gamma^1{}_{42}\right) + \left(\boxed{\Gamma^2{}_{44}}\Gamma^2{}_{22} - \Gamma^2{}_{24}\Gamma^2{}_{42}\right) + \left(\boxed{\Gamma^2{}_{44}}\Gamma^3{}_{32} - \boxed{\Gamma^2{}_{34}}\Gamma^3{}_{42}\right) + \left(\boxed{\Gamma^2{}_{44}}\Gamma^4{}_{42} - \boxed{\Gamma^2{}_{44}}\Gamma^4{}_{42}\right) \\ + \left(\boxed{\Gamma^3{}_{44}}\Gamma^1{}_{13} - \boxed{\Gamma^3{}_{14}}\Gamma^1{}_{43}\right) + \left(\boxed{\Gamma^3{}_{44}}\Gamma^2{}_{23} - \boxed{\Gamma^3{}_{24}}\Gamma^2{}_{43}\right) + \left(\boxed{\Gamma^3{}_{44}}\Gamma^3{}_{33} - \Gamma^3{}_{34}\Gamma^3{}_{43}\right) + \left(\boxed{\Gamma^3{}_{44}}\Gamma^4{}_{43} - \boxed{\Gamma^3{}_{44}}\Gamma^4{}_{43}\right) \\ + \left(\Gamma^4{}_{44}\Gamma^1{}_{14} - \boxed{\Gamma^4{}_{14}}\Gamma^1{}_{44}\right) + \left(\Gamma^4{}_{44}\Gamma^2{}_{24} - \boxed{\Gamma^4{}_{24}}\Gamma^2{}_{44}\right) + \left(\Gamma^4{}_{44}\Gamma^3{}_{34} - \boxed{\Gamma^4{}_{34}}\Gamma^3{}_{44}\right) + \left(\boxed{\Gamma^4{}_{44}\Gamma^4{}_{44} - \Gamma^4{}_{44}\Gamma^4{}_{44}}\right) \end{bmatrix}$$

$$R_{44} = -\left[\partial_4\Gamma^1{}_{14} + \partial_4\Gamma^2{}_{24} + \partial_4\Gamma^3{}_{34}\right] + \left[\left(-\Gamma^1{}_{14}\Gamma^1{}_{41}\right) + \left(-\Gamma^2{}_{24}\Gamma^2{}_{42}\right) + \left(-\Gamma^3{}_{34}\Gamma^3{}_{43}\right) + \left(\Gamma^4{}_{44}\Gamma^1{}_{14}\right) + \left(\Gamma^4{}_{44}\Gamma^2{}_{24}\right) + \left(\Gamma^4{}_{44}\Gamma^3{}_{34}\right)\right]$$

$$R_{44} = -\frac{3}{2}\partial_4{}^2\ln\psi(x_4) + \begin{bmatrix} -\left(\frac{1}{2}\partial_4\ln\psi(x_4)\right)^2 - \left(\frac{1}{2}\partial_4\ln\psi(x_4)\right)^2 - \left(\frac{1}{2}\partial_4\ln\psi(x_4)\right)^2 \\ + \left(\frac{1}{2}\partial_4\ln\psi(x_4)\right)^2 + \left(\frac{1}{2}\partial_4\ln\psi(x_4)\right)^2 + \left(\frac{1}{2}\partial_4\ln\psi(x_4)\right)^2 \end{bmatrix} \rightarrow \boxed{R_{44} = -\frac{3}{2}\partial_4{}^2\ln\psi(x_4)}$$

$$\boxed{R_{11} = R_{22} = R_{33} = \frac{1}{2}\partial_4{}^2\ln\psi(x_4) + \frac{1}{2}\left(\partial_4\ln\psi(x_4)\right)^2 \ , \ R_{44} = -\frac{3}{2}\partial_4{}^2\ln\psi(x_4)}$$

APPENDIX 4.

$$R_{11}-\frac{1}{2}Rg_{11}=\kappa p$$
$$R_{11}-\frac{1}{2}R\psi(x_4)\eta_{11}=\kappa p$$
$$\frac{1}{2}\partial_4{}^2\ln\psi(x_4)+\frac{1}{2}\left(\partial_4\ln\psi(x_4)\right)^2\ -\frac{1}{2}\left(3\partial_4{}^2\ln\psi(x_4)+\frac{3}{2}\left(\partial_4\ln\psi(x_4)\right)^2\right)\psi^{-1}(x_4)\psi(x_4)\eta_{11}=\kappa p$$
$$\boxed{-\partial_4{}^2\ln\psi(x_4)\ -\frac{1}{4}\left(\partial_4\ln\psi(x_4)\right)^2=\kappa p}$$

$$R_{44}-\frac{1}{2}Rg_{44}=\kappa\left(\varepsilon_p+\varepsilon_s\right)$$
$$R_{44}-\frac{1}{2}R\psi(x_4)\eta_{44}=\kappa\left(\varepsilon_p+\varepsilon_s\right)$$
$$-\frac{3}{2}\partial_4{}^2\ln\psi(x_4)-\frac{1}{2}\left(3\partial_4{}^2\ln\psi(x_4)+\frac{3}{2}\left(\partial_4\ln\psi(x_4)\right)^2\right)\psi^{-1}(x_4)\psi(x_4)\eta_{44}=\kappa\left(\varepsilon_p+\varepsilon_s\right)$$
$$\boxed{\frac{3}{4}\left(\partial_4\ln\psi(x_4)\right)^2=\kappa\left(\varepsilon_p+\varepsilon_s\right)}$$

APPENDIX 5.

E3 - space

$$\left.\begin{array}{l}\partial_1 g_{\mu\nu}\left(x_4\right)=0\\ \partial_2 g_{\mu\nu}\left(x_4\right)=0\\ \partial_3 g_{\mu\nu}\left(x_4\right)=0\end{array}\right\}\rightarrow R_{\lambda\nu}=\partial_\mu\Gamma^\mu{}_{\nu\lambda}-\partial_\nu\Gamma^\mu{}_{\mu\lambda}+\Gamma^\eta{}_{\nu\lambda}\Gamma^\mu{}_{\mu\eta}-\Gamma^\eta{}_{\mu\lambda}\Gamma^\mu{}_{\nu\eta}=0\rightarrow\boxed{R=0}$$

APPENDIX 6.

$$g_{\mu\nu}=\psi(x_4)\eta_{\mu\nu}$$
$$g^{\mu\nu}=\psi^{-1}(x_4)\eta^{\mu\nu}$$
$$R_{11}=R_{22}=R_{33}=\frac{1}{2}\partial_4{}^2\ln\psi(x_4)+\frac{1}{2}\left(\partial_4\ln\psi(x_4)\right)^2\ ,$$
$$R_{44}=-\frac{3}{2}\partial_4{}^2\ln\psi(x_4)$$
$$R=R_{\mu\nu}g^{\mu\nu}=R_{\mu\nu}\eta^{\mu\nu}\psi^{-1}(x_4)=\left(R_{11}+R_{22}+R_{33}-R_{44}\right)\psi^{-1}(x_4)=\left(3\partial_4{}^2\ln\psi(x_4)+\frac{3}{2}\left(\partial_4\ln\psi(x_4)\right)^2\right)\psi^{-1}(x_4)$$
$$R=\left(3\partial_4{}^2\ln\psi(x_4)+\frac{3}{2}\left(\partial_4\ln\psi(x_4)\right)^2\right)\psi^{-1}(x_4)$$
$$\psi_\pm(x_4)=e^{\left[\pm x_4\sqrt{\frac{4}{3}\kappa\left(\varepsilon_p+\varepsilon_s\right)}\right]}\geq 0$$
$$\Rightarrow\left\{\begin{array}{l}R=\left(\underbrace{3\partial_4{}^2\ln\left(e^{\left[\pm x_4\sqrt{\frac{4}{3}\kappa\left(\varepsilon_p+\varepsilon_s\right)}\right]}\right)}_{0}+\frac{3}{2}\left(\partial_4\ln\left(e^{\left[\pm x_4\sqrt{\frac{4}{3}\kappa\left(\varepsilon_p+\varepsilon_s\right)}\right]}\right)\right)^2\right)\psi_\pm{}^{-1}(x_4)\\ \boxed{R\left(\psi_\pm(x_4)\right)=2\kappa\left(\varepsilon_p+\varepsilon_s\right)\psi_\pm{}^{-1}(x_4)\geq 0}\end{array}\right.$$